A Set of Topological Graphs for 2-D Sensor Ad Hoc Networks

Tarek El Salti and Nidal Nasser
Department of Computing and Information Science
University of Guelph, Ontario, Canada
Email: telsalti@uoguelph.ca, nasser@cis.uoguelph.ca

Tarik Taleb
Graduate School of Information Sciences
Tohoku University, Sendai, Japan
Email: talebtarik@ieee.org

Abstract—**Recently, different types of sensors have been developed to detect many unexpected environmental changes (e.g., instability of the earth's crust) that have been occurred. Thus, reducing the massive destruction (e.g., Tsunamis) that may occur from those changes. However, the sensor technology used needs to be improved in terms of several design factors (e.g., topology and sensing-coverage). In this paper, we focus on the underlying topology in sensor networks in two-dimensional environments and propose a new set of graphs referred to as the Derived Circles (DC^α) graphs. We show that these graphs are locally constructed, connected, power efficient, and orientation-invariant. We also show that these graphs have a minimum degree of one and an Euclidean dilation of one. Furthermore, via simulations, we demonstrate that the DC^α graphs outperform the Half Space Proximal (HSP) graph in terms of the network dilation, Euclidean dilation, and power dilation. This, in turn, reduces the energy consumption of the nodes and accordingly prolong the network lifetime.**

I. Introduction

Climate changes and unstable earth's crust are effecting the World environment. Oceans are one environmental component that has heavily affected by those factors. An example would be the recent instability of the earth's crust in ocean floors, which affects the Oceans in creating high and dangerous wave lengths (e.g., Tsunamis 2004). In response to these disasters, different sensors have been developed to improve the detection level of these disasters.

A sensor node can send and receive message (packet) to/from its neighbouring node if these nodes are within their transmission range of each other. However, because each sensor node is restricted by its limited resources (i.e., its battery power), the communication range [3], [4] between this node, and its neighbouring nodes is limited. Therefore, even though a node and its intended destination may not be within the transmission range of each other, these nodes can still communicate via the routing functionality; i.e., forwarding the packet along the path between a node and its intended destination via their intermediate nodes (hops).

There are various topological graphs used in sensor networks. These topologies exist to determine the neighbouring nodes of a given node. Among all the topologies, the Unit Disk Graph (UDG) is a common graph that has been widely used. Unfortunately, routing on UDG is not efficient, since UDG is a dense graph with a high average node degree. As a result, running routing protocols based on UDG takes considerable time. Another drawback is that routing on UDG does not work all the time, since the UDG topology is typically a non-planar topological graph with crossing edges. These crossing edges cause some routing protocols (e.g., Face routing protocol [18]) to fail in delivering data packets. As a result, several sub topological graphs [8], [17] of UDG have been proposed to deal with its drawbacks. Implementing and running routing protocols on the proposed topologies improve their performance. However, some topologies still have some limitations. For example, they are not orientation-invariant: if a graph (G) is rotated by an arbitrary angle to form the graph (G'), then the resulting sub topological graph of G' ($P(G')$) is not necessarily a rotation of the sub topological graph of G ($P(G)$). Therefore, running a a routing protocol on $P(G)$ may yield different results compared to the same routing protocol running on $P(G')$. This actually affects the accuracy of the routing protocol evaluation and thus misjudges the routing protocol performance.

Hence, one of the primary concerns in the area of sensor networks is to develop algorithms that control the network topologies [13], [14]. Due to the fact that sensor nodes are operated by limited battery power, have limited amount of memory, and have topologies that are often not available and may be dynamic, localized algorithms with prior knowledge on neighboring nodes up to a fixed number of hops away, are ideally preferred. The reason for choosing these algorithms is that they have the following properties that deal with the sensor network limitations: 1) Bounding node degrees [16], 2) Planarity [5], 3) Low weight (the weight of a graph is close to the weight of the Euclidean minimum spanning tree) [12], 4) Power efficiency [11], and 5) Bounding the stretch factors [10].

There are various topological graphs ([8], [17]) that were constructed based on these localized algorithms. We are mainly interested in the recently proposed graph, which is referred to as the Half Space Proximal (HSP) graph [8]. The reason for choosing this graph, is that it is considered a new graph compared to some other proposed graphs [17]. Moreover, the HSP graph is proposed for ad hoc networks in general, which can apply to sensor networks. In addition, since the energy consumption is of great concern in sensor networks, and since there is no performance evaluation for the HSP in terms of power, we would like to demonstrate experimentally

the HSP performance in terms of power dilation.

Generally, several topological graphs have been proposed in the literature in the context of ad hoc networks, where the sensor network is a one type of the ad hoc networks, and they are as follows. The work done by Yao [17] proposes a topological graph, referred to as the *Yao Graph* $YG_k(G)$ (also called a *Theta Graph* [7]) with an integer parameter k, where $k \geq 6$ and G is a geometric graph. We first define a directed Yao graph, $D\text{-}\vec{Y}G_k(G)$, for G as follows. At each node u in G, k equally-separated rays originating at u define k cones. In each cone, only the directed edge (u,v) to the nearest neighbor v, if any, is part of $D\text{-}\vec{Y}G_k(G)$. Ties are broken arbitrarily. Let $YG_k(G)$ be the undirected graph obtained if the direction of each edge in $D\text{-}\vec{Y}G_k(G)$ is ignored, yielding a subgraph which may have crossing edges if $G = UDG$. The graph $YG_k(G)$ is a $1/(1 - 2sin(\pi/k))$-spanner of G [11], has an out-degree of at most k, and contains the Euclidean Minimum Spanning Tree ($EMST(G)$) as a subgraph [17]. One drawback of the $YG_k(G)$ graph is that it is not orientation-invariant.

Another work by Chavez *et al.* [8] proposes a topological graph referred to as the *Half Space Proximal Graph HSP(G)*, where G is a geometric graph, and it is defined as follows. As with the *Yao Graph*, first a directed $D\text{-}\vec{H}SP(G)$ is defined. At each node u in G, the following iterative procedure is performed until all the neighbors of u are either discarded or are connected with an edge. A directed edge (u,v) is formed with the nearest neighbor v. An open half plane is defined by a line perpendicular to (u,v), intersecting (u,v) at its midway point, and containing v. All the nodes in this half plane are then discarded. The procedure then continues with the next nearest non-discarded neighbor and so on until all the nodes have been discarded. The selected directed edges determine the $D\text{-}\vec{H}SP(G)$. The undirected $HSP(G)$ is obtained by ignoring the direction of the edges, yielding a subgraph that may still have crossing edges. Among the properties shown in [8] for the HSP subgraph are the following: it is strongly connected, has an out-degree of at most six, has a stretch factor of at most $(2\pi + 1)$, contains the $EMST(G)$ as its subgraph, and is orientation-invariant. Bose *et al.* [6] show that this stretch factor of at most $2\pi + 1$ is incorrect and that no upper bound is known although the stretch factor is at least $(3-\epsilon)$ [6]. One drawback of the $HSP(G)$ graph is that, since the forbidden region is always defined by a straight line, there is no control over the degree of a node.

Recently, Bose et al. [6] introduced a family of directed geometric graphs, related to the HSP, that depend on two parameters θ and λ. For $0 \leq \theta < \pi/2$ and $1/2 < \lambda < 1$, their graph is a strong t-spanner, with $t = 1/((1\text{-}\lambda) cos(\theta))$. The out-degree of a node is at most $\lfloor (2\pi/(min(\theta, arccos(1/2\lambda)))) \rfloor$.

In this paper, we propose a new topological graph which is referred to as the Derived Circle (DC^α). Afterwords, we generalize the definition of the DC^α graph to define a set of orientation-invariant DC^α graphs which include the UDG graph as a special case. This set of graphs permits the control over the degree of the nodes while being orientation-invariant. Acquiring this property preserves the accuracy of the routing

protocol performance evaluation regardless of the rotation of the nodes. Furthermore, reducing the degree of nodes increases the speed of the routing decisions performed on the DC^α graph. However, the DC^α graph does not remove too many edges, since there is a need for these edges to improve the different kind of dilations (e.g. Euclidean dilation).

Moreover, the DC^α graphs are shown to be connected graphs, have a node degree of at least one, and have an Euclidean dilation of at least one. In addition, we empirically demonstrate that the DC^α graphs outperform the HSP in terms of the network, Euclidean, and power dilations. Thus, the length of the shortest path between any pair of nodes in the DC^α topologies is shorter than the shortest path between the same pair of nodes in the HSP. Therefore, less energy consumed when forwarding a message in the DC^α's paths, which leads to an increase in the lifetime of a sensor network. In addition, acquiring shorter paths implies faster message delivery. All these properties strictly impact the performance of any routing protocol that runs on the DC^α topologies.

The rest of the paper is organized as follows. In Section II, we define the concepts that are partially used in our solution. In Section III, we illustrate the proposed solution by introducing the Derived Circle (DC^α). Furthermore, we explore its properties theoretically. In Section IV, we experimentally demonstrate the DC^α's properties. Finally, concluding remarks are drawn in Section V.

II. PRELIMNARIES

Before presenting our new set of graphs, we first demonstrate some of the geometric concepts and metrics that are needed as a part of our solution. Moreover, we explore the model that encompasses our new topological graphs.

A. Geometric Concepts and Metrics

In our communication model, a graph on the point set S in 2-D, can be modeled as a weighted (undirected or directed) graph $G(S,E)$ where E is the set of edges (u,v) between nodes u and $v \in S$. The weight of an edge (u,v) is the 2-D Euclidean distance $|uv|$. The weight of a graph is the sum of its edge weights. Moreover, in our model, two nodes u and v, where $u \neq v$, are connected by an undirected edge if the Euclidean distance between them is at most their transmission range (R_c). The resulting graph is called a Unit Disk Graph (UDG). For each node u, we denote the set of its neighbors by $N(u)$. The number of the neighbors of u is the degree of u.

Define a subgraph of G, $P(G)$, as a t-spanner of G if the length of the shortest path between any two nodes in $P(G)$ is at most t times the shortest path between them in G, where t is the stretch factor. The length of a path is divided into three main types: 1) Euclidean path length, 2) network path length, and 3) power path length [11]. The first type refers to the sum of all the hops' Euclidean distances in a path. The second type refers to the hop count of a path. The last type refers to the sum of the consumed energy for the edges in a path referred by $p(\pi) = \sum_{i=1}^{q} ||v_{i-1}v_i||^\beta$, where π refers to
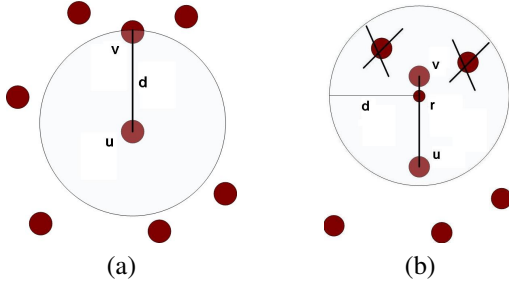
(a)   (b)

Fig. 1. (a) DC^α graph is constructed where $\alpha = 0$. (b) DC^α graph is constructed where α is close to one.

the path, q refers to the total number of nodes, v_i refers to a sensor node, and β is a constant parameter from within the interval $[2, 5]$.

The stretch factor is represented by the dilation. Adopting the definition in [], the shortest path in UDG in terms of Euclidean is $|uv|$, in terms of hops is $\left\lceil \frac{|uv|}{R_c} \right\rceil$, and in terms of power is $|uv|^\beta$.

B. Network Model

Although our network model applies to any kind of environments, we are interested in deploying the network model in underwater environments (e.g., oceans, lakes, rivers), specifically ocean floors. Deploying the new and existing subgraphs of UDG on ocean floors allows us to study the instability of the earth's crust in ocean floors. This increases the level of prediction of any dangerous wave lengths, which therefore, saves more lives. However, we assume that the sensor nodes are fixed and their 2-D positions are known via some positioning techniques proposed in [2].

III. DESCRIPTION AND ANALYSIS OF DERIVED CIRCLE (DC^α) GRAPHS

In this section, we give formal definition of the proposed Derived Circle (DC^α) graphs and present some of their properties. Before presenting the new graph, we first assume that S is a set of N nodes in the Euclidean two dimensional plane, where each node possessing a geometric location. Each node u running the DC^α algorithm (see Algorithm 1) will pick a neighbor, v, from the list of neighbours, $N(u)$, that is the nearest neighbouring node to u. Afterwords, a restricted forbidden area (i.e., circle) is drawn on u with a radius d, where d is the distance between u and v. The circle eliminates any edge with a neighbor q, where $q \neq v$, that falls into the circle. We repeat the same process for each sensor node. We use the term α to parameterize the closed line segment between u and v: $(1-\alpha)u + \alpha v$, $0 \leq \alpha \leq 1$. Any particular choice of α represents the position of the circle position between u and v. This is illustrated in Figure 1. Notice that in Figure 1a, the centre of the circle is located at node u. Also notice that the circle in Figure 1b is centered at the point r and the edge between the current node and its nearest neighbor is preserved while eliminating other edges.

The definition of the $D - DC^\alpha$ is summarized as follows.

Algorithm 1 $DC^\alpha(G, \alpha)$ graph algorithm.

Input: *A graph G with the node set S, and a parameter α.*
Output: *A list of undirected/directed edges L for each node $u \in S$ which represent the DC^α subgraph of G, $DC^\alpha(G)$.*
for all $u \in S$ **do**
    Create a list of neighbors of u: $LN(u) = N(u)$. $L = \phi$
    repeat
        (a) Remove the nearest neighbor v node from $LN(u)$ and add the undirected/directed edge (u , v) to L.
        (b) Let $r = (1 - \alpha)u + \alpha v$ be a point on the line segment uv.
        (c) Scan the list $LN(u)$ and remove each node in the interior of the circle drawn at position r with a radius d, where d is the distance between u and v.
    until $LN(u)$ is empty
end for

Definition 1: Let G be a UDG with node set S. The directed D-DC^α subgraph is defined as the graph with node set S whose edges are obtained by applying the $DC^\alpha(G)$ algorithm (Algorithm 1) on the graph G using displacement parameter α.

Referring to the above definition, the undirected graph $DC^\alpha(G)$ is obtained by ignoring the direction of the edges in D-DC^α. In this paper, we are interested in the undirected version. However, when setting $\alpha = 0$ or even with a very small value, we simply refer to the resultant graph as the UDG graph. This can be explained as follows (see Algorithm 1). When α is very small or equal to zero, the $DC^\alpha(G)$ may not eliminate edges, since there will be no neighbouring node, z, closer to node u than node v. Notice that the directions of the nearest neighbor does not effect the construction of the DC^α graphs. Therefore, the resultant subgraph is the same regardless of the orientation of the point set S. Hence, the $DC^\alpha(G)$ is orientation-invariant. The running time of Algorithm 1 per node is $O(l^2)$ where l is the degree of the node. After giving detailed description of the DC^α graphs, along with the orientation-invariant property, we show additional properties for the DC^α graphs as follows.

Theorem 1: Consider a node set L and UDG defined on L. The minimum degree of the DC^α graph, when $\alpha = 0$, is at least one.

Proof: Assume that the current node A (See Figure 2) has neighbors Nei(A)= ($N1...Nr$), where $r = \infty$, such that each neighbor Ni, where $1 \leq i \leq \infty$, is of a distance of R_c from node A. According to the DC^α graph, node A will pick one of the neighbors, assume $N1$, therefore, node A will remove the edges with the other neighbors $N2...Nr$ (Nei(A)={$N1$}). Moreover, nodes $N2...Nr$ will never insert node A in their list of neighbors since node A is not the nearest neighbor for $N2...Nr$. Hence, one edge is created from node A to node $N1$, which means that node A can have a degree of one. ∎

Theorem 2: Consider a node set L and UDG defined on L. If $UDG(L)$ is connected, then DC^α graphs, where $0 \leq \alpha \leq 1$, is also connected.
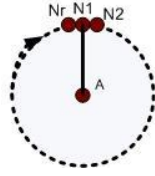
Fig. 2. DC^α subgraph, where $\alpha = 0$. The rotated arrow indicates that there are surrounding neighbors.
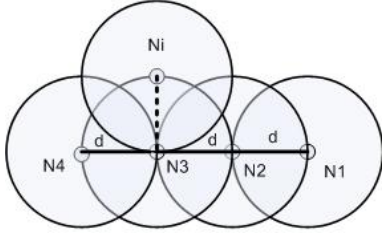

Fig. 3. Proof for Theorem 2, where $\alpha = 0$. The circles refer to the restricted forbidden area in the DC^α graphs.

Proof: Assume n is the total number of nodes L. If n=1, then it is trivial that the DC^α subgraph is connected. Assume for $n > 1$, the subgraph is connected. We want to show that the subgraph is connected when $\exists\, n+1$ nodes. From Figure 3, we have a connected DC^α subgraph with n nodes[1]. Adding a new neighbor with a distance of d to any of the nodes in the figure, assuming new node Ni is a neighbor of the node $N3$ would imply that Ni has an undirected edge $(N3,Ni)$. Since the DC^α graph is connected when $\exists\, n$ nodes, therefore, the DC^α graph is still connected when $\exists\, n + 1$ nodes. ∎

Theorem 3: Consider a node set L and UDG defined on L. The Euclidean stretch factor for DC^α, where $0 \leq \alpha \leq 1$, is at least 1.

Proof: Assume the following: a) $\alpha = 0$, b) The circle drawn in the DC^α subgraph contains no other nodes except the nearest neighbor, and c) the term n is the total number of nodes L (See Figure 4). Since the DC^α subgraph is always connected (according to Theorem 2), there is always a path between any pair of nodes u, v, where $u \neq v$. Following the assumption (b), the edges are all preserved without leading to any edge removal. Therefore, all the paths in DC^α would be identical to those in UDG. Hence, leading to an Euclidean stretch factor of one. ∎

IV. PERFORMANCE EVALUATION

In this section, we evaluate the performance of the DC^α graphs and compare them to HSP graph [8]. To demonstrate the evaluation procedure, we first present the simulation model used along with the evaluation metrics. Later, we show the obtained simulation results.

A. Simulation Model

In our experiments, we used randomly chosen connected Unit Disk Graphs (UDG) on an area of 100×100. We varied

[1]Assume that the distance d between a node and its neighbors is equal to R_c.
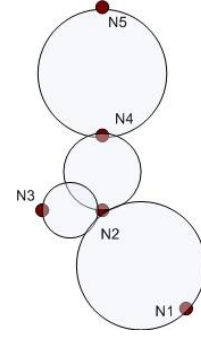

Fig. 4. The proof for Theorem 3. The circles refer to the transmission range R_c

the number of nodes, n, between 65, 75, 85, 95, and 105 nodes. For each UDG, DC^α graphs with $\alpha = 0$, $\alpha = 0.25$, $\alpha = 0.50$, $\alpha = 0.75$, $\alpha = 1.0$, and HSP are all generated. We set the transmission range R_c to 15 units in all tested graphs.

B. Performance Evaluation Metrics

There are two main metrics used in our experiments. The first metric is called the dilation and it is defined as follows. Having a graph G, we define a subgraph of G, $P(G)$, as a t-spanner of G if the length of the shortest path between any two nodes in $P(G)$ is at most t times the shortest path between them in G, where t is the stretch factor. The length of a path is divided into three main types: 1) Euclidean path length, 2) network path length, and 3) power path length [11]. The first type refers to the sum of all the hops' Euclidean distances in a path. The second type refers to the hop count of a path. The last type refers to the sum of the consumed energy for the edges in a path referred by $p(\pi) = \sum_{i=1}^{q} ||v_{i-1}v_i||^\beta$, where π refers to the path, q refers to the total number of nodes, v_i refers to a sensor node, and β is a constant parameter from within the interval $[2, 5]$.

The stretch factor is represented by the dilation. Adopting the definition in [], the shortest path in UDG in terms of Euclidean is $|uv|$, in terms of hops is $\left\lceil \frac{|uv|}{R_c} \right\rceil$, and in terms of power is $|uv|^\beta$. In this paper, we set β to two. However, we study the upper and average bounds for the network, Euclidean, and power dilations in order to know their average and worst cases. The second metric used is the average node degree, where the node degree refers to the number of neighbors for a node.

C. Simulation Results

From Figure 5, it is shown that even though the DC^α graphs, where $0 \leq \alpha \leq 1$, do not outperform the HSP in terms of the average node degree, they still outperform the UDG. In particular, the DC^α graphs perform much better when $\alpha > 0$. This is because as α increases, the circle drawn in the DC^α has more chances to eliminate more edges. However, as α reaches the value of one, the DC^α is still being able to remove edges, but at the same time, there is a possibility that the circle does not anymore contain some neighboring nodes

that they used to be in the circle when α is smaller. This explains why the DC^α graphs, when $\alpha = 0.5, 0.75, 1$, are very close to each other in terms of the average node degree.
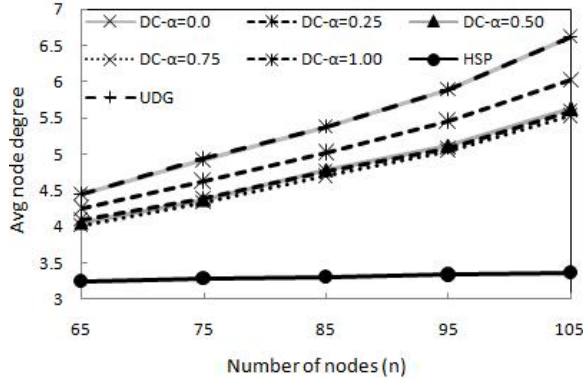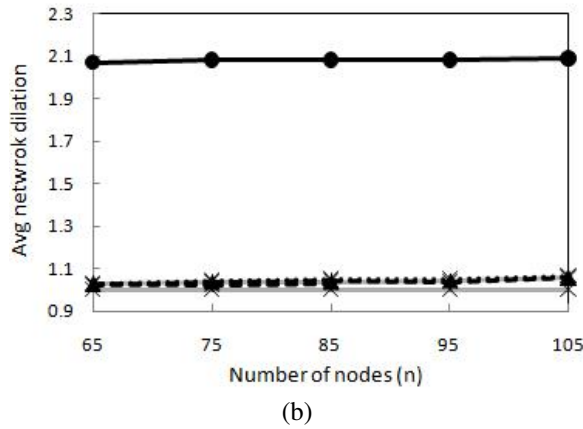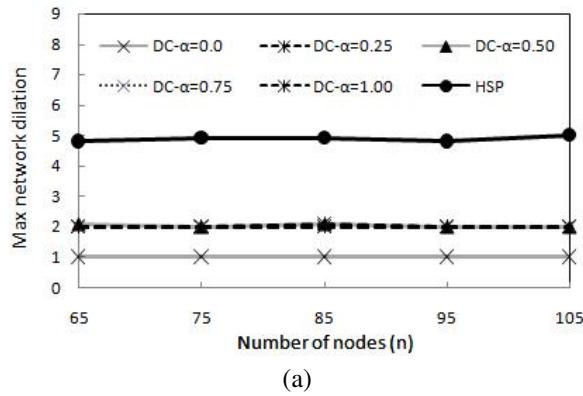

Fig. 5.   Average node degree.

(a)

(b)

Fig. 6.   (a) Maximum network dilation. (b) Average network dilation.

From Figures 6 and 7, the DC^α graphs outperform the HSP graph in terms of network and Euclidean dilations (both maximum and average dilations). This can be seen through all the values of α. We explain this behavior based on Figure 5 as follows. As α increases, the DC^α graphs eliminate more edges, but since those graphs deal with a forbidden restricted area (i.e., circle), they do not eliminate too many edges as HSP does. Therefore, more edges exist in the DC^α graphs.
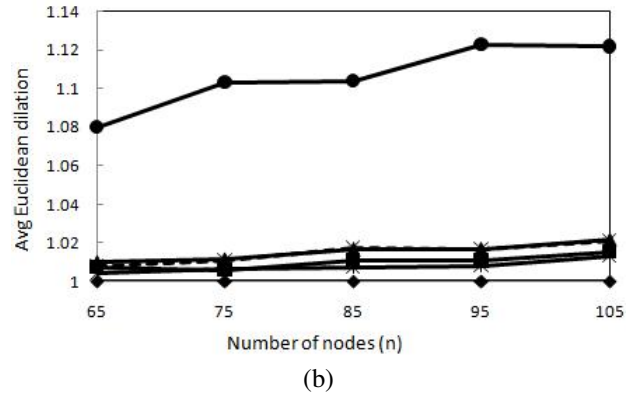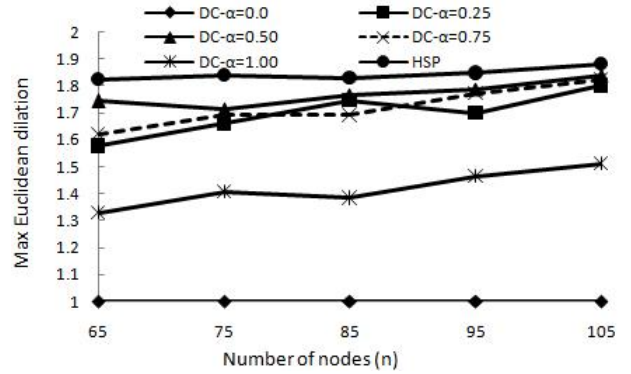

(a)

(b)

Fig. 7.   (a) Maximum Euclidean dilation. (b) Average Euclidean dilation.

This implies that the DC^α graphs have higher possibility to find shorter paths than those that exist in the HSP graph. However, there is another interesting behavior for the DC^α graphs, which is clearly shown in Figure 7 (especially the maximum dilation). As α increases, the dilation increases, and reaches its maximum value at $\alpha = 0.5$. However, when $\alpha > 0.5$, there is a reflection in the DC^α's behavior; i.e., the dilation decreases. The reason for this behavior is that as α overpasses the midpoint between the current node and its nearest neighbor, the circle drawn starts to loose some nodes that were in the interior of the circle, and thus constructing more edges. Hence, there is a higher possibility to find shorter paths than those that exist in DC^α graphs, where $0 < \alpha \le 0.5$.

One point to mention is that when $\alpha = 0$, the maximum and the average Euclidean dilations for the DC^α graph is equal to one, which adequately verify Theorem 3. Another point to mention is that from our experiments, we found that all the tested DC^α graphs, where $0 \le \alpha \le 1$, always remain connected. Thus, Theorem 2 is adequately verified.

As can be seen from Figure 8 (both maximum and average dilations), the DC^α graphs outperform the HSP in terms of the power dilation. This is due to the fact that the DC^α graphs, where $0 \le \alpha \le 1$, have smaller Euclidean dilations than the HSP (See Figure 7). This means that the DC^α graphs, where $0 \le \alpha \le 1$, consume less energy (i.e., battery power) of the sensor nodes than the HSP graph does. Thus, prolonging the life of the network.
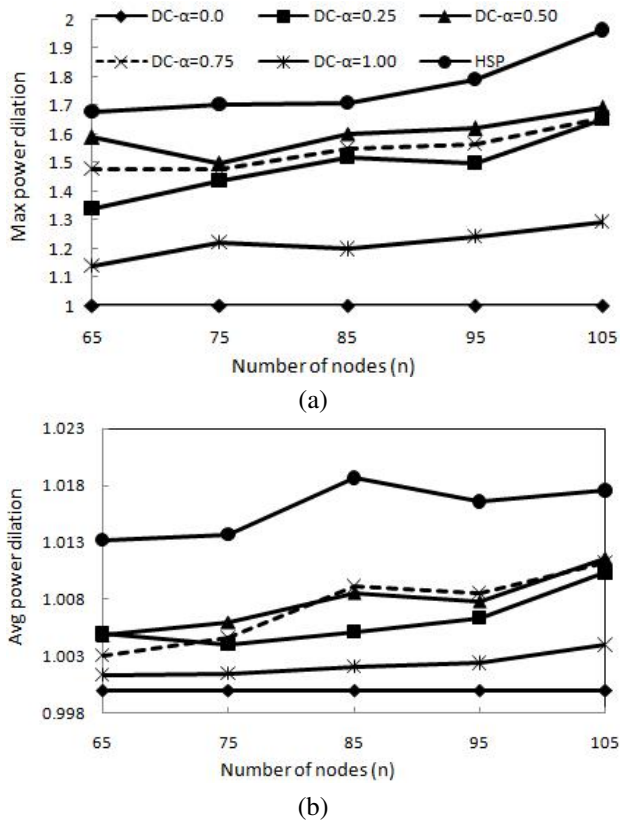
Fig. 8. (a) Maximum power dilation. (b) Average power dilation.

V. CONCLUSIONS

In this paper, we proposed a set of topological graphs which are referred to as the Derived Circle (DC^α), where α represents the position of the forbidden restricted area between a node and its nearest neighbor. This allows us to control the degree of the nodes. Moreover, we have shown that the DC^α graphs are locally constructed, connected, power efficient, and orientation-invariant. Furthermore, we demonstrated experimentally that the DC^α graphs outperform HSP in terms of the network, Euclidean, and power dilations with low values. Achieving low network dilation improves any routing protocol that will run on the DC^α graphs in terms of the time messages need to be delivered to the destinations. Furthermore, achieving low Euclidean dilation also improves the time for message delivery. This verifies the previous results obtained when measuring the network dilation. In addition, achieving low Euclidean dilation strictly means that the energy spent for transmitting a message from one sensor node to another is low. This reduces the energy consumption of the overall sensor networks, which therefore, prolongs the lifetime of the network. Lastly, it is obvious that when achieving low power dilation, the energy consumption would be low. This verifies the results obtained when measuring the Euclidean dilation.

As a result of this study, we have found that the DC^α graphs are power and time efficient topologies for sensor ad hoc networks. Additionally, these topologies will obviously impact the routing protocols that will run on top of them. The reason is that, since the dilations are of a great concern for the routing protocols (e.g., [15]), and because the new topologies achieved low dilations, the routing protocols will be dramatically improved when they run on top of these topologies. For future work, we will extend all the work from 2-D to 3-D environments.

REFERENCES

[1] I. F. Akyildiz, D. Pompili, and T. Melodia Underwater acoustic sensor networks: research challenges. *in Ad Hoc Networks Journal (Elsevier)*, Vol. 3, No. 3, pages 257–279, Mar. 2005.

[2] V. Chandrasekhar, W. KG Seah, Y. Sang Choo, and H. Voon Ee. Localization in underwater sensor networks: survey and challenges. *in Proceedings of the 1st ACM international workshop on Underwater networks*, pages 33–40, Los Angeles, CA, USA, Sept. 2006.

[3] L. Barrière, P. Fraigniaud, L. Narayanan, and J. Opatrny. Robust position-based routing in wireless ad hoc networks with irregular transmission ranges. *in Wireless Communications and Mobile Computing Journal*, Vol. 3, No. 2, pages 141–153, 2003.

[4] S. Basagni, I. Chlamtac, V.R. Syrotiuk, and B.A. Woodward. A distance routing effect algorithm for mobility (DREAM). *in Proc. of 4th ACM/IEEE Conference on Mobile Computing and Networking (Mobicom '98)*, Dallas, Texas, United States, Oct. 1998.

[5] P. Boone, E. Chavez, L. Gleitzky, E. Kranakis, J. Opatrny, G. Salazar, and J. Urrutia. Morelia test: Improving the efficiency of the Gabriel test and face routing in ad-hoc networks. *in Proc. of SIROCCO '04*, Smolenice Castle, Slovakia, June 2004.

[6] P. Bose, P. Carmi, M. Couture, M. Smid, and D. Xu. On a family of strong geometric spanners that admit local routing strategies. *in Proceedings of the Workshop of Algorithms and Data Structures (WADS)*, pages 300–311, Portland, Oregon, USA, 2007.

[7] P. Bose, J. Gudmundsson, and P. Morin. Ordered theta graphs. *Computational Geometry: Theory and Applications*, Vol. 28, No. 1, pages 11–18, May 2004.

[8] E. Chavez, S. Dobrev, E. Kranakis, J. Opatrny, L. Stacho, H. Tejeda, and J. Urrutia. Half-space proximal: A new local test for extracting a bounded dilation spanner. *in Proc. of the International Conference On Principles of Distributed Systems (OPODIS 2005), vol. 3974 of LNCS*, pages 235–245, Pisa, Italy, 2006.

[9] R. Cayirci, H. Tezcan, Y. Dogan, and V. Coskun. Wireless sensor networks for underwater survelliance systems. *in Ad Hoc Networks Journal (Elsevier)*, Vol. 4, No. 4, pages 431–446, July 2006.

[10] X.-Y. Li, G. Călinescu, and P.-J. Wan. Distributed construction of a planar spanner and routing for ad hoc wireless networks. *in Proc. of INFOCOM'2002*, Vol. 3, pages 1268–1277, 2002.

[11] X.-Y. Li, P.-J. Wan, and Y. Wang. Power efficient and sparse spanner for wireless ad hoc networks. *in Proc. of IEEE Int. Conf. on Computer Communications and Networks (ICCCN01)*, pages 564–567, Scottsdale, AZ, USA, 2002.

[12] X.-Y. Li, Y. Wang, P.-J. Wan, W.-Z. Song, and O. Frieder. Localized low-weight graph and its applications in wireless ad hoc networks. *in Proc. of Twenty-Third IEEE INFOCOM 2004*, pages 610–628, Hong Kong, China, March 2004.

[13] X.Y. Li. *Topology Control in Wireless Ad Hoc Networks*. IEEE Press, 2003.

[14] R. Rajaraman. Topology control and routing in ad hoc networks: A survey. *ACM SICACT News*, Vol. 33, No. 2, pages 60–73, June 2002.

[15] T. El Salti, T. Fevens, and A.E. Abdallah. Fast Progress-Based Routing in Sensing-Covered Networks. *To appear in the Proc. of the IEEE Global Communications Conference (GLOBECOM)*, New Orleans, LA, USA, Dec. 2008.

[16] Y. Wang, X.-Y. Li, and O. Frieder. Distributed spannar with bounded degree for wireless ad hoc networks. *in International Journal on Foundations of Computer Science*, Vol. 14, No. 2, pages 183–200, 2003.

[17] A.C.-C. Yao. On constructing minimum spanning trees in k-dimensional spaces and related problems. *in SIAM Journal on Computing*, Vol. 11, No. 4, pages 721–736, Nov. 1982.

[18] P. Bose, P. Morin, I. Stojmenovic, and J. Urrutia. Routing with guaranteed delivery in ad hoc wireless networks. *in Wireless Networks*, vol. 7, No. 6, pages 609–616, November 2001.